Comprehensive two-dimensional liquid chromatography – high-resolution mass spectrometry for complex protein digest analysis using parallel gradients

Rick S. van den Hurk [a,b,1], Bart Lagerwaard [a,b,1], Nathan J. Terlouw [a,b], Mingzhe Sun [a,b], Job J. Tieleman [a,b], Anniek X. Verstegen [a,b], Saer Samanipour [a,b], Bob W.J. Pirok [a,b] , Andrea F.G. Gargano [a,b*]

[a] *Analytical Chemistry Group, Van 't Hoff Institute for Molecular Sciences, University of Amsterdam, The Netherlands*

[b] *Centre for Analytical Sciences Amsterdam (CASA), the Netherlands*

[1] These authors contributed equally

* Corresponding author

Andrea F.G. Gargano a.gargano@uva.nl

Keywords: two-dimensional liquid chromatography, parallel gradients, protein digest analysis, high-resolution mass spectrometry

Abstract

Despite the high gain in peak capacity, online comprehensive two-dimensional liquid chromatography coupled with high-resolution mass spectrometry (LC×LC-HRMS) has not yet been widely applied to the analysis of complex protein digests such as cell lysates. One reason is the reduced sensitivity of the methods, with second separation dimensions that run at high flow rates, resulting in the need for flow splitters to couple to MS and inducing high dilution factors.

This study reports proof of principle results of the development of a LC×LC-HRMS using parallel gradients for the analysis of complex digests, removing the need for post-column splitting pre-MS with reduced flow rates in the second dimension (0.7 $mL \cdot min^{-1}$). With this strategy, high 2D surface coverage and peak capacity were obtained (peak capacity of 679 in 60 minutes). The analysis of human cell culture lysate digest by parallel RPLC×RPLC MS/MS resulted in the identification of 8959 peptides and 1984 proteins within 1hr run. This was a gain of 149% in the number of peptides identified compared to 1D-LC method. Parameters such as the gradient program, flow rate and modulation time were investigated. This approach reduces the complexity of gradient programming as two simple linear gradients can be programmed in both dimensions, eliminating the need for column re-equilibration between different modulations, making it attractive for LC×LC methods at low flowrates. Prospectives on the limits and application of such methods are discussed.

1. Introduction

Modern liquid chromatography (LC) high-resolution mass spectrometry (HRMS) instruments reach scan rates of over 40 Hz allowing for fast analysis and fragmentation expreriments. This makes LC-HRMS the method of choice to study changes in the proteome of complex

organisms and to characterize the sequence of proteins, such as biotherapeutics. [1–3]. In these experiments, proteins are digested into peptides (bottom-up proteomics) and LC separations are essential to resolve the tens of thousands of peptides in a sample [4]. The separation quality thus significantly influences the speed and depth of bottom-up proteomics analysis [5]. The metric most often used to describe the quality of a LC separation is the peak capacity, approximating the maximum number of peaks that can be resolved at an equal resolution within a given separation space [6]. Ultra-high-pressure LC technology commonly allows for peak capacity between 100 and 200 per hour [7]. For the analysis of highly complex samples, comprehensive two-dimensional LC (LC×LC) is an attractive option as it can offer one order of magnitude higher peak capacity [8–11]

Combining two different retention mechanisms that target unique chemical properties of the analytes (*e.g.* charge and hydrophobicity) result in orthogonal methods and efficiently use the separation space in both dimensions [9]. In the past years, LC×LC has been applied for separating protein digests or other peptide mixtures, using e.g. ion exchange [12], hydrophilic interaction chromatography (HILIC) [13–16], mixed mode [17] chromatography and reversed-phase liquid chromatography (RPLC) [18]. However, the combination of such selectivities can yield solvent-compatibility issues that may jeopardize the separation[9].

Therefore, a commonly applied selectivity combination is RPLC×RPLC [19]. This combination yields fundamentally limited orthogonality yet provides excellent solvent compatibility between the dimensions and high-resolution separations. The most common methods either employ different column chemistries (*e.g.* [20]) or combine basic mobile phases in the first dimension (^{1}D) with acidic RPLC in the second dimension (^{2}D) [21]. Nevertheless, the still limited orthogonality of the two separations principally results in low retention space coverage when using full gradients in the ^{2}D separation. For this reason, shifted gradients can be used where the ^{2}D mobile phase gradient method is correlated to the gradient program in ^{1}D

to maximize the surface coverage [9]. Using this approach Stoll *et al.* reached a peak capacity of 10,000 in 4 hrs for the analysis of a monoclonal antibody digest [21]. Despite high-performance, the use of shifted gradients has also been criticized. Chapel *et al.* [22] found that the increase in retention space coverage and peak capacity is obtained at the expense of sensitivity and retention time repeatability in consecutive 2D separations.

Moreover, the most critical disadvantage of any repeating gradient (i.e. shifted or full) in LC×LC is that high flow rates are required to minimize dwell and column equilibration time. For hyphenation with MS, post-column flow splitting is thus required, which significantly reduces the sensitivity of the resulting method[23]. Consequently, LC×LC thus far has been considered not attractive for complex protein digest analysis.

One alternative to shifted gradients to extend the usage of the 2D separation space in LC×LC is the use of parallel gradients. With this approach, in the second dimension separation, a single gradient with a slope correlated to the first dimension (hence "parallel") is programmed throughout the analysis. Parallel gradients have been investigated since 2007, demonstrating that this method can improve the use of available ^{2}D separation space in correlated RPLC×RPLC platforms [24–26]. In 2020 Aly *et al.* [27] demonstrated that the potential of correlated LC×LC systems was maximized by using parallel gradients as opposed to full- and shifted-gradient programs. Parallel ^{2}D gradients in RPLC×RPLC have so far been applied in proof of principle experiments for the separation of pharmaceuticals [27], food [24,28], and simple aromatic compounds [29]. An additional advantage is that not using repeated ^{2}D gradients results in more constant pressure on the ^{2}D column, which minimizes physical stress on both the column and other system components [30].

Moreover, parallel gradients do not require high ^{2}D flow rates and consequently omit the need for post-column flow splitting when hyphenating to MS. Flow splitting has several downsides. As recently described by Gunnarson *et al.* [23], smaller analyte peak volumes are

more susceptible to dispersion in connecting capillaries between the split point and the detector. The authors found significantly increased peak width (even up to double peak with for small molecules with high diffusion coefficients) when split flow was used. To achieve high MS sensitivity, flow splitting is thus preferably avoided.

In this work, the use of parallel gradients RPLC×RPLC is exploited to achieve high retention-space coverage and peak capacity for peptide separations. Additionally, high separation capacity of LC×LC was achieved, while flow-splitting is avoided. First, the stationary phases for the ^{1}D and ^{2}D were selected by 1D-LC experiments. These were used to develop a parallel gradient program. The modulation time was reduced to explore the effect on undersampling, effective peak capacity, wrap-around, sensitivity, and retention-space coverage. Finally, the method was compared with a 1D-LC separation of the same analysis time and assessed based on peak capacity, retention-space coverage and identified peptides and proteins by MS/MS.

2. Experimental

2.1 Chemicals

Water (ULC/MS –CC/SFC grade), 2-propanol (HPLC grade) and acetonitrile (ACN, LC-MS grade) were obtained from Biosolve (Valkenswaard, The Netherlands). Dichloromethane (DCM) was obtained from VWR chemicals (Fontenay-sous-Bois, France). Ammonium bicarbonate (Bioultra, ≥ 99.5%) was acquired from Fluka Analytical (Charlotte, USA). Formic acid (FA, ≥98%) was acquired from Analar Analytical (Amsterdam, The Netherlands).

Liquid nitrogen, argon (AR, 5.0) gas and helium (HE) gas were obtained from Praxair (Guildford, UK). Alpha casein (≥ 70.0%), bovine serum albumin (BSA, lyophilised powder, ≥ 96%), myoglobin (from equine heart, essentially salt-free, lyophylized powder, ≥ 90% (SDS-

PAGE)), albumin (from chicken egg white, lyophilized powder, ≥98%, agarose gel electrophoresis), urea (≥ 98%), trypsin (BRP grade), trifluoroacetic acid (TFA, ≥ 99.0%, HPLC grade), thiourea (puriss. p.a., ACS reagent, ≥ 99.0%), Humanized IgG1k Monoclonal Antibody (NIST, Lot: 14HB-D-002;) were all obtained from Sigma (Zwijndrecht, The Netherlands). Human IMR90 lung fibroblast cells (ATCC CCL-186) were prepared according to what was described in [31]. Solid-phase extraction (SPE) was performed with C18 cartridges (Supelco; 1 mL, 100 mg bed, pore size 70 Å)

2.2 Instrumentation

All experiments in this study were carried out using an Agilent 1290 series Infinity 2D-LC system (Agilent, Waldbronn, Germany). The system comprised of two binary Infinity I pumps (G4220A), one 1100 isocratic pump (G1310A), an autosampler (G4226A), a thermostatted column compartment (G1316C) and a valve drive (G1170A), equipped with an 8-port 2-position 2D-LC valve (G4236A) and a diode-array detector (G4212A) with Agilent Max-Light cartridge cells (G4212-60008, 10 mm, V-det = 1.0 µL). The system was controlled using Agilent OpenLAB CDS Chemstation Edition (Version 3.2 (Build 3.2.0.620)) software. The ^{1}D column was an Agilent InfinityLab Poroshell 120 EC-CN (50×2.1mm, 2.7 µm). The ^{2}D column was a ZORBAX Eclipse Plus C18 (50×2.1mm, 1.8 µm). In addition a Phenomenex Kinetex F5 (150×2.1mm, 1.7 µm), Agilent ZORBAX Eclipse Plus Phenyl-Hexyl (50×4.6mm, 1.8 µm) and a Waters Acquity UPLC BEH Glycan column (150×2.1mm, 1.7 µm particles) were used.

For 2DLC experiments using SPAM, two Phenomex SecurityGuard™ ULTRA C18 Cartridges (2×2.1mm) were used with the corresponding Phenomex SecurityGuard™ ULTRA Holders as traps. The mass spectrometer used was an Q Exactive Plus (Thermo Scientific, Bremen, Germany).

2.3 Procedures

2.3.1 Sample preparation

The sample preparation is based on previously described work by Roca *et al.* [32]. The detailed procedure is described in the Supporting Information (SI) Section S-1. A protein digest sample consisting of BSA or 4 different proteins (BSA, α-casein, myoglobin and albumin) was used for method development. A cell lysate, was used to prove the applicability of the method (Human IMR90 lung fibroblast cells).

In short, the proteins were digested overnight at 37 °C using trypsin. The next day, the sample was desalted using C18 SPE. Lastly, The peptide solution was freeze-dried and reconstituted in H_2O/ACN (98/2, v/v) with 0.1% TFA to a theoretical concentration of 1 mg mL^{-1} for analysis.

2.3.2 1D-LC-MS

For all 1D-LC experiments the ^{1}D column was directly connected to the MS source. The injection volume was 5 µL, column thermostat was 50°C and the sample compartment 7°C. Mobile phase A consisted of H_2O/ACN (98/2, v/v), mobile phase B was H_2O/ACN (20/80, v/v). to both mobile phases, 0.1% FA was added. The electrospray ionization (ESI) MS were done positive ion mode at a resolution setting of 70.000 for full scan mode (300 to 1600 m/z) and 17.500 for MS^2 mode. The source conditions were varied depending on the flow rate of the LC effluent, at low flow rates, a capillary voltage of 2.5 kV was applied whereas from 0.4 mL min^{-1} and above a voltage of 3.5 kV was applied. Sheath gas flow rate and capillary- and gas temperatures were increased with increasing flow rate. A full overview of the used MS settings is presented in the SI Section S-2 Tables S1-S3.

For the scanning gradient experiments, both the C18 and CN column were used [33]. In all experiments a flow rate of 0.2 mL min^{-1} was employed. All three gradients were set to

have a 2-minute hold of 2% B, then linearly increased to 50% B over either 5, 15, or 45 minutes, followed by a 3-minute hold at 50% B before returning to start conditions. To determine the optimal conditions to use in ^{1}D for 2D-LC, multiple 1D-LC experiments were performed on the CN column with varying flow rates (0.03, 0.06, and 0.12 mL min^{-1}) and ACN concentrations (from 2 to 50% B or to 30% B). For the comparison of 1D-LC with 2D-LC, 1D-LC experiments with the C18 column and a flow rate of 0.7 mL min^{-1} were performed (gradients ending either at 30% B or 25% B). The exact gradient programming for all of these experments can be found in the SI Section S-3 Tables S4-S6.

2.3.3 On-line RPLC×RPLC-MS

Sample, solvent composition (of both ^{1}D and ^{2}D separations), column temperature and MS settings were the same as described in the previous section. For the 2D-LC experiments, the ^{1}D column was CN and the ^{2}D column was C18. A schematic overview of the system is depicted in Figure S1 of Section S-5 in the SI. 10 µL of sample was injected. In all cases where the ^{1}D flow rate was 0.03 mL min^{-1}, the ^{1}D gradient was programmed in the following steps: 0-2-60-65-70-70.01 min and respectively 2-2-50-90-90-2 for the percentage of B. Using a ^{1}D flow rate of 0.06 mL min^{-1}, the gradient was altered such that the percentage of B was 30 instead of 50 at the third time step (2-2-30-90-90-2). A lower gradient slope was used to maintain peak spreading over the full 60-minute gradient time, while double the gradient volume was used, before the wash step at 90% B.

For initial optimization of the parallel gradient, the ^{2}D gradient was programmed in the following steps: 0-5-65-70-70.01 min and respectively 2-2-50-90-2 for the percentage of B. different offsets were tesed where steps 1, 2, 3 and 5 were increased to start at 5, 10, 15, and 20% B. Following this experiment, a multi-step ^{2}D gradient was proposed which was programmed as follows: 0-5-15-30-65-70-70.01 min and respectively 8-8-16-20-48-90-8% B.

This gradient programming was used to compare ^{2}D flow rates of 0.4 and 0.7 mL min^{-1}. Later the same programming was used at varied modulation times of 1, 0.67, 0.57, 0.5, 0.3, and 0.25 min at a ^{2}D flow rate of 0.7 mL min^{-1} to study the effect of modulation time on effective peak capacity and retention-space coverage.

For the final method, the ^{1}D flow rate was set at 0.06 mL min^{-1} using the same gradient as described above. The ^{2}D gradient was adjusted accordingly to the following steps: 0-8-27-65-70-70.01 minutes at respectively 8-12-22-40-90-8% B.

2.3.4 Data handling

Plotting the chromatograms and performing retention modelling calculations was performed using the MOREPEAKS software [34]. Peptide and protein identification was performed in MaxQuant (V2.1.0.0). Carbamidomethyl was used as a fixed modification and the variable modifications were set to oxidation and acetylation. Trypsin was specified as the enzyme, with a maximum of two missed cleavages. The false discovery rate (FDR) for the peptide identification was set to 1%. Other calculations were performed using MATLAB R2021a. MS data was converted in msConvert 3.0 to mzXML. MZmine60 version 2.53 was used for feature detection from LC and LCxLC-MS experiments. Details can be found in the SI Section S-4. Raw data are available at https://massive.ucsd.edu/ProteoSAFe dataset MSV000092199.

3. Results and Discussion

3.1 Selectivity screening for column selection

To allow for parallel gradients method to be effective, the two separation dimensions must be partially correlated but feature different selectivities (*e.g.* elution order of analytes) [24,27]. Therefore, the first step of our investigation was the evaluation of different column chemistries and mobile phase combinations for their suitability to be applied in a parallel RPLC×RPLC

setup. Using a BSA digest as representative peptide sample, we monitored 31 peptides features (the list of m/z features is reported in Table S8) and investigated the orthogonality to assess the correlation between different reversed-phase selectivities. Five different reversed-phase selectivities were investigated: i) C18 using ACN as organic modifier, ii) C18 using MeOH as modifier, iii) cyano functionality, iv) phenyl-hexyl functionality, and v) pentafluorophenyl (PFP) functionality. In Figure 1, a subset of the orthogonality plots are presented by plotting the normalized retention time (ntr) of a specific analyte for each selectivity against each other and their correlation was calculated as R^2-value (see Figure S2 for all comparisons to C18 ACN). Lower R^2-value represents lower correlation and therefore, higher orthogonality of the compared selectivities. As a demonstration of highly orthogonal systems, a HILIC separation was added and shown in Figure 1C, resulting in an R^2-value of 0.2138. The correlation between the C18 MeOH, phenyl-hexyl, and PFP was very similar, with R^2-values around 0.98 for all three cases. The lowest correlation between the RPLC selectivities was obtained by combination with the cyano-based stationary-phase chemistry, in which changes of normalized retention as well as elution order were observed. Therefore, the combination of C18 and cyano stationary phases using ACN as modifier was further investigated.

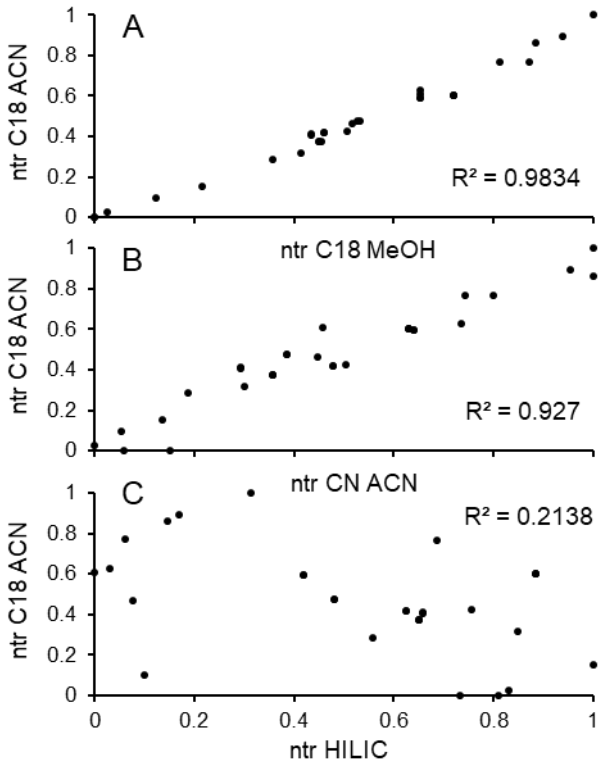

226

227 Figure 1: Orthogonality plots using normalized retention times (ntr) of a subset of targeted
228 peptide features. The following three comparisons are presented: C18 using ACN modifier (y-
229 axis in all subplots) vs C18 MeOH (A), cyano (B), and HILIC (C).
230

231 Retention modelling was used to investigate the retention behavior of the two selected
232 mechanisms and determine which selectivity should be used as first-dimension separation
233 mechanism. Scanning-gradient experiments, as described by den Uijl *et al.* [33], of 5, 15, and
234 45 minutes were performed on both columns. Subsequently, retention modelling using the
235 linear-solvent-strength (LSS) model was performed using MOREPEAKS [34], to model the
236 relationship between the retention factor (k) and organic modifier fraction (φ). Based on this
237 LSS model, Figure 2 was constructed where the natural logarithm of k at a specific φ was
238 plotted for each targeted peptide feature that was investigated. In these plots, the slope is related
239 to the interaction of the analyte and the modifier for that specific stationary-phase chemistry.
240 The slopes observed using the C18 column (Figure 2B) are steeper than those observed using
241 the cyano column (Figure 2A). Moreover, higher retention was observed for the C18 column

as for each peptide a higher φ was required for elution. Moreover, the peak capacity (n_c) of the C18 method was higher respect to the CN ($n_{c,CN}$ = 77 and $n_{c,C18}$ = 89, for a 30 min gradient, other data in Figure S3). From these data, we concluded that the C18 chemistry was a better candidate for ^{2}D separation as: i) it allowed for better focusing conditions (higher φ was required for elution), ii) it offered higher peak capacity, iii) the steep ln k vs φ curves underlined a more pronounced "on-off" retention mechanism. The latter indicated that the analytes will only elute in a small window of % of organic modifier, with limited to no elution under isocratic or very shallow gradients. These conditions should ensure good separation capacity under the shallow gradient conditions that will be used in the ^{2}D separation in parallel gradients.

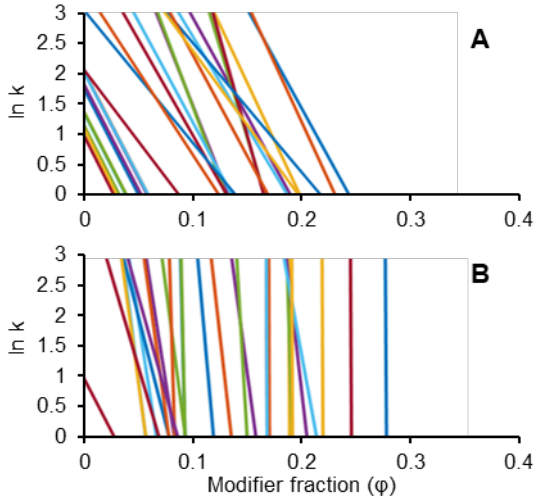

Figure 2: Retention-modelling plots constructed using the MOREPEAKS software by applying the LSS model to scanning-gradient data of targeted peptides for the cyano column (A) and the C18 column (B). The list of m/z features used reported in Table S8.

3.2 Development of the parallel-gradient LC×LC method

3.2.1 Parallel gradient method development

In passively modulated full-gradient or shifted-gradient LC×LC systems, focussing may take place at the head of the ^{2}D column depending on the gradient programming. This effect is less pronounced in parallel LC×LC methods due to its near-isocratic elution conditions in the low

260 *k* range. Previous research on parallel gradients development underlined the negative effect of
261 injection band broadening on the method's peak capacity [24]. To overcome this, recent
262 research applied dilution flow prior collections into loops, improving analyte focusing [27]. In
263 our investigation, we diluted the ^{1}D eluent to enable refocussing on trap columns, also known
264 as stationary-phase-assisted modulation (SPAM) to better focus the analyte fraction from the
265 ^{1}D separation prior to injection in the shallow ^{2}D gradients. SPAM strategies have the
266 advantage of allowing the collection high modulation volumes from the ^{1}D effluent, reducing
267 their volumes [35]. In our experiments, this (i) reduced the injection volume and solvent
268 strength of the fractions from the ^{1}D separation, allowing to use of narrow internal diameter
269 (2.1 mm) in the ^{2}D separation, (ii) facilitated the use of lower volumetric flow rates in the ^{2}D
270 separation (0.4-0.7 mL min^{-1}) eliminating the need for post-column splitting prior MS
271 coupling, (iii) facilitated increasing the linear flow velocity in the ^{1}D separation, reducing the
272 dead time and increasing the use of 2D space. Overall this was helpful to reduce dilution and
273 increase sensitivity in LC×LC-MS [36].
274 As concluded above from the retention models of the two columns, the ^{2}D column
275 requires a higher φ for elution than the ^{1}D column. For this reason, the ^{2}D gradient should be
276 positively offset compared to the ^{1}D gradient. Initially, a series of parallel gradients were
277 investigated with different φ offsets as depicted in Figure 3A, a 1 min ^{2}D modulation time was
278 used (0.4 mL min^{-1}) and a 60 min ^{1}D gradient (0.03 mL min^{-1}). A protein digest sample
279 consisting of 4 different proteins (BSA, A-casein, myoglobin and albumin) was used to
280 evaluate the method. Multiple ^{2}D gradients were evaluated, having 5 min of hold time to
281 compensate for the ^{1}D dwell volume and varying from 2 to 20% the initial %B to a final
282 composition between 50 and 70% were compared. In particular, the results of the ^{2}D gradients
283 2-50% and 10-60% B are discussed (their 2D-LC chromatograms are depicted in Figure S4A
284 and S4B). Notably, the gradient starting at 2% B resulted in high ^{2}D retention and wider

peakwidths (e.g. 0.163 min FWHM) for analytes having a ^{1}D elution before 25 minutes while showing lower retention and narrower peakwidths (e.g. 0.054 min FWHM) for those eluting after 25 minutes. The opposite effect was observed for the gradient starting at 10% B, resulting in a good ^{2}D separation up to 25 minutes and almost exclusively elution at the ^{2}D t_0 time after 25 minutes. We observed that, if the ^{2}D retention is too high (e.g. elution after 5 column volumes), peak broadening occurs as peakwidths and elution time go back to what it was in the 1D-LC C18-RPLC.

It was concluded that a multi-step parallel gradient should be investigated, such as the one depicted in Figure 3B to ensure all analytes experience relatively low retention in the ^{2}D separation. The proposed multi-step gradient was also investigated with a few small (2% B) offsets and demonstrated good separation for all analytes across the 60-minute separation space as shown in Figure 4A.

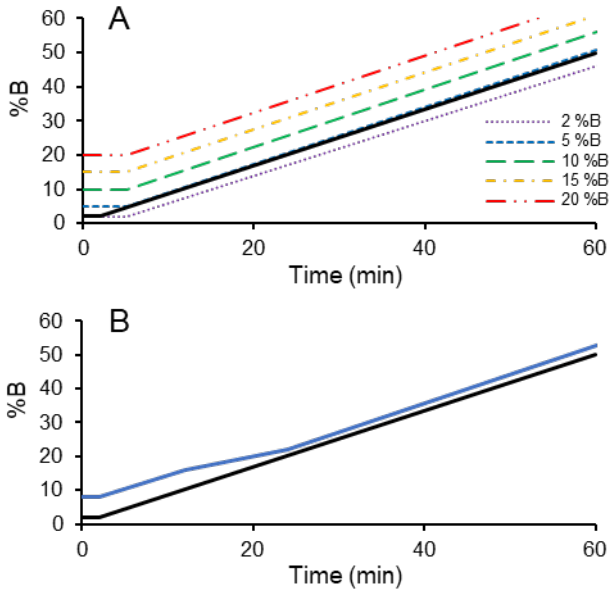

Figure 3: Initial parallel-gradient programming with constant ^{1}D gradient (black) and a series of ^{2}D gradients with varying φ offsets starting at 2, 5, 10, 15, and 20 %B (blue lines) (A), and a multi-step ^{2}D parallel gradient (B).

3.2.2 *Method optimization: effect of flow rate and modulation time*

Parallel gradients can reduce modulation times as no ^{2}D gradient delivery and column re-equilibration are required. Shorter modulation times are beneficial to prevent so-called undersampling of the ^{1}D to maintain high effective peak capacity. On the contrary, when too short modulations are used, a possible consequence is that the analytes are not yet eluted from the ^{2}D column during the modulation time, leading to what is commonly reffered as "wrap-around" [27]. Utilizing wrap-around may be beneficial when it comes to increasing the use of available retention space. However, as every modulation is performed using nearly isocratic elution conditions in the ^{2}D, high ^{2}D retention may lead to broader peaks, resulting in lower overall effective peak capacity.

In our optimization, we focused on reducing the modulation time and evaluated the effect of this on the use of separation space and method peak capacity. As first step, the ^{2}D flow rate was increased from 0.4 mL·min^{-1} to 0.7 mL· min^{-1}, the maximum for MS hyphenation in our MS system without post-column flow splitting. The resulting chromatogram is presented in Figure 4B. Using 0.7 mL· min^{-1}, all peaks elute at lower time in the ^{2}D separation (mostly below 40 s) and with narrower ^{2}D peak widths (0.035 and 0.054 min FWHM for 0.7 and 0.4 mL·min^{-1}, respectively). This condition was selected for further optimization.

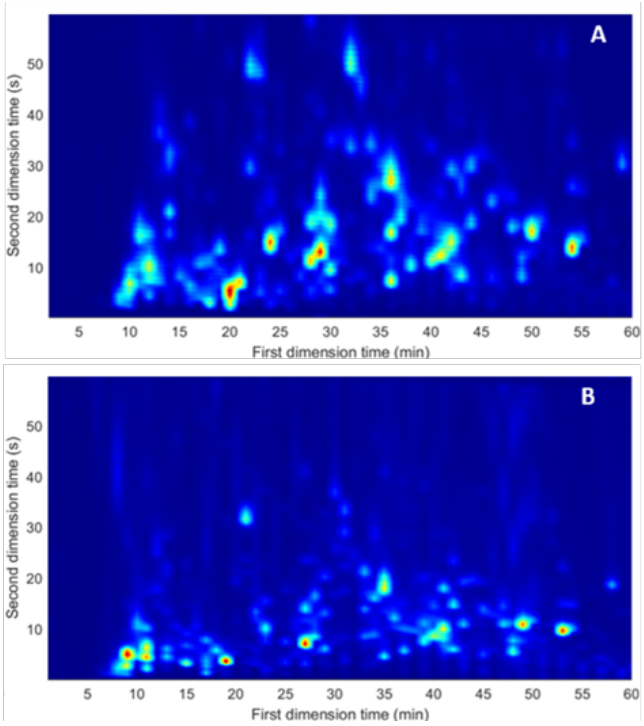

Figure 4: TIC chromatograms of a multi-step ^{2}D parallel gradient at ^{2}D flow rate of 0.4 mL min^{-1} (A) and 0.7 mL min^{-1} (B).

Next, the modulation times were programmed as 1, 0.67, 0.57, 0.5, 0.30 and 0.25 minutes and the undersampling, wrap around and surface coverage is described in Table 1 and in the next sections. To evaluate the results obtained the number of modulations in which targeted features (Table S9) appeared were counted to assess the extent of undersampling. Furthermore, the β factor for undersampling can be calculated per modulation time to correct theoretical peak capacity to effective peak capacity [37].

3.2.2.1 Undersampling

Figure 5 depicts the number of times a ^{1}D peak was sampled for different modulation times based on the same 36 selected features as above (see SI Section S-6 Figures S5, S6, and S7 for all modulation times and the corresponding LC×LC chromatograms). As can be seen, higher sampling frequencies are realized by shorter modulation times. Ideally, the first

dimension was sampled 2 to 3 times to mitigate the loss of the first dimension peak capacity [38]. However, over-sampling the ^{1}D leads to further sample dilution and loss in effective peak capacity (Table 1). Oversampling was more pronounced at 0.25 and 0.3 minute modulation times, where the average maximum intensity per feature was reduced by at least 30% compared to a 1-minute modulation time (Table 1). Based on these principles, 0.57 minutes appears as most attractive because most features were sampled 2 or 3 times.

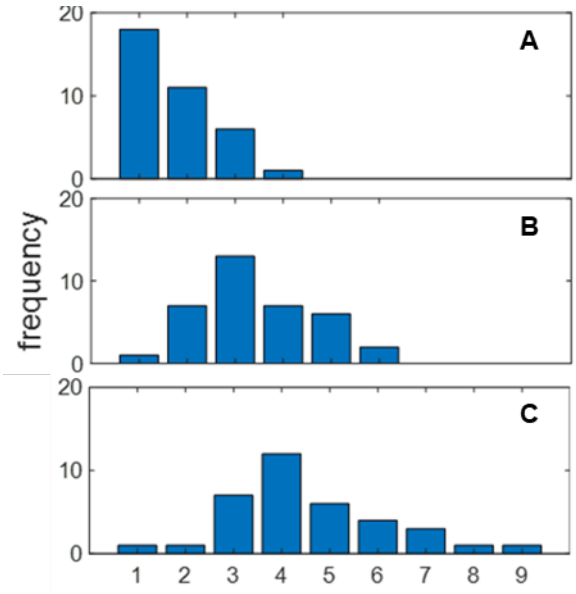

Figure 5: The number of times a ^{1}D peak was sampled by the ^{2}D per modulation time (A: 1 min, B: 0.57 min, and C: 0.25 min) for 36 features.

3.2.2.2 Wrap around, surface coverage, peak capacity analysis

Another aspect that can be considered, and is exclusively available in parallel gradients, is to use wrap-around to increase the retention-space coverage. This is common practice in GC×GC applications but rarely explored and often undesired in LC×LC applications [27,39]. Aly *et al.* [27] demonstrated that as long as peak co-elution with successive fractions was avoided, wrap-around lead to the most efficient utilization of the separation space. The degree of wrap-around and the retention-space coverage were calculated based on 196 most intense

common features between these six measurements. For retention-space coverage (RSC), the bin-counting approach was used with a 14 by 14 grid (196 bins, equal to the number of features) [40]. In our analysis, no normalization of retention times was applied for both the ^{1}D and ^{2}D in order to account for the time in which no analyte elution was occuring. The calculated retention-space coverages for modulation times are reported in Table 1, the retention-space coverage tend to increase with decreasing modulation time.

To estimate the presence of wrap-around due to modulation time reduction, we used the data of the same 196 features monitored in 1-minute modulation time as a reference. For all the modulation times, the data was extracted as ^{2}D retention time, corrected for ^{2}D dead time (0.29 min) (as displayed also in Figures S6 and S7). Features were flagged as wrap-around candidate if their ^{2}D retention time in the 1-minute modulation experiment was larger than the modulation time for the current experiment. For example, when estimating the degree of wrap around for 0.5 min modulation time, it was calculated as the number of features experiencing ^{2}D elution time >0.5 divided by the total number of features (196) (Figure S8). Table 1 summarizes all the metrics used to evaluate the methods using different modulation times. It shows that no significant wrap around (<0.5% of total features) is expected with modulation times down to 0.5 min. When the modulation time is reduced to 0.3 or 0.25 min, 13.8% and 19.4% of features are expected to experience wrap around. It is not desirable to have excessive wrap-around taking place as it risks artificially splitting peaks in different ^{2}D retention times. From our data we selected a modulation time of 0.57 min as it seemed to be the best balance between sensitivity (maximal peak intensity), effective 2D peak capacity (combined effect of reduction in undersampling, β, and increase in ^{2}D peak width with decreasing modulation times) and retention-space coverage without excessive wrap-around.

Table 1: Comparison of different modulation times by several performance indicators including the expected percentage of wrap around, the undersampling factor (β), ^{2}D peak

intensity, ^{2}D peak capacity (^2n_c), effective 2D peak capacity ($n'_{c,2D}$), and retention-space coverage by bin counting.

Modulation time (min)	wrap around (%)*	β	^{2}D Intensity ($\cdot 10^8$ counts)**	^{2}D FWHM (min)**	^2n_c**	$n'_{c,2D}$**	RSC*
1	0	3.21	3.79	0.0354	17.62	548.86	0.2194
0.67	0	2.28	3.24	0.0328	13.02	572.11	0.2857
0.57	0.5	2.01	3.61	0.0355	10.45	520.76	0.3061
0.5	0.5	1.82	3.01	0.0380	8.75	479.70	0.3163
0.3	13.8	1.36	2.42	0.0391	5.52	407.08	0.3469
0.25	19.4	1.26	2.02	0.0472	4.12	327.64	0.3469

* based on 196 features.as described in materials and methods.

** based on 36 features from Table S9.

3.3 Application of parallel CN×RPLC-HRMS to the analysis of complex protein digest

Prior analysis of a complex cell lysate digest, we increased the ^{1}D flow rate from 0.03 mL min^{-1} to 0.06 mL min^{-1} to increase the usable separation space, reducing the impact of the dwell and dead time of the ^{1}D separation. This can be applied in the setup as SPAM allows concentrating the factions collected from the 1D effluent and injecting a constant volume in the ^{2}D separation. Figure 6A displays the TIC signal for the protein mix digest using the final method. The use of 0.06 mL min^{-1} in the ^{1}D allowed to have the first peaks eluting before at about 3.2 minutes (about 6.5 min were needed for the 0.03 mL min^{-1} method) and separation performance was maintained.

As final step we applied the CN×RPLC-HRMS method to analyze a human fibroblast digest and compared to 1D-RPLC C18 separations. A 2DLC base-peak-chromatogram of the separation of the cell digest is shown in Figure 6B (1D representation in Figure S9A). Despite the parallel gradient being optimized on peptides originating from a mixture of four proteins, similar use of the separation space was observed with a more complex sample. 2D peak capacity of 679 in 60 minutes (average peak width of about 6 s) was achieved whereas a relative

to a peak capacity of 134 was achieved in the 1D method (average peak width of about 20 s) (see Figures S9B and S9C). With correction for undersampling using β, a peak capacity of 373 was achieved. By performing 2D-LC using parallel gradients, the effective peak capacity was increased by a factor 2.8 compared to 1DLC.

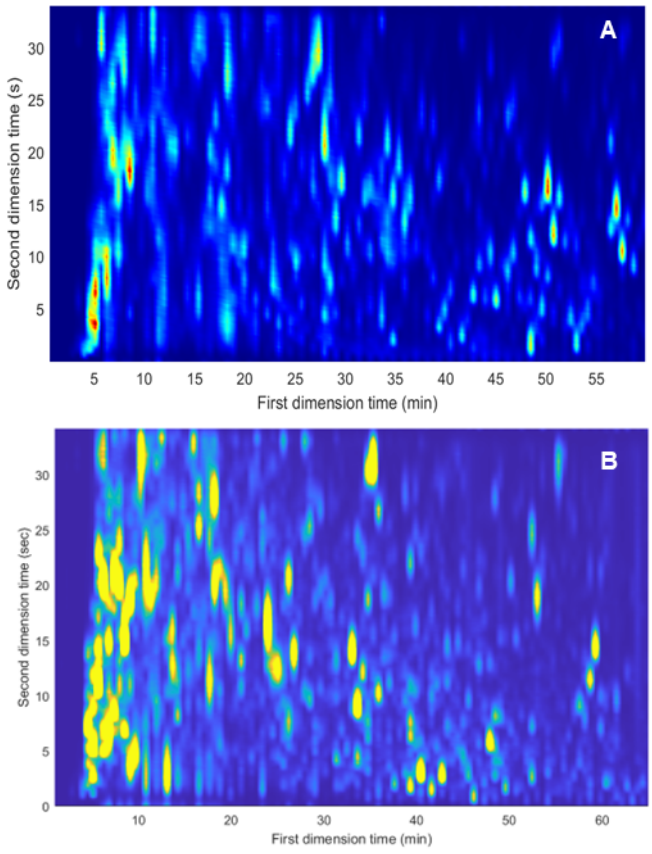

Figure 6: Total-ion chromatogram of the digested protein mixture using the optimized LC×LC method (A). base-peak chromatogram of the IMR90 cell lysate digest (B).

To further evaluate the usefulness of the extra separation power and retention-space coverage, we analyzed the results from peptide identification by MS/MS. Using parallel-gradient RPLC×RPLC-MS/MS, 8959 peptides and 1984 proteins were identified with a false discovery rate (FDR) of 1% for the 1D-LC-MS/MS of the same sample, 6014 peptides and 1250 proteins were identified, offering an improvement of roughly a factor 1.5 in the number of proteins identified within the same analysis time.

4. Conclusions

This study demonstrates that efficient parallel gradients in RPLC×RPLC separations of complex peptide samples can be achieved and coupled to MS without the use of flow splitting. Some of the advantages of these methods are (i) the efficient use of the available separation space due to the absence of ^{2}D gradient-equilibration time, (ii) simpler method development compared to shifted-gradient approaches and (iii) avoiding the abrupt changes in solvent composition typical of fast gradients, reducing mechanical stress to ^{2}D columns and ESI-MS signal perturbation.

In our proof of principle method, an effective peak capacity of 373 was obtained for a cell-digest sample. It should be noted that our main focus was to maintain MS sensitivity avoiding post-column flow splitting. While we used effective peak capacity as a factor for optimization and comparison of the methods, our aim was to maximize MS and MS/MS feature analysis per unit time by utilizing higher retention-space coverage and maintaining detection sensitivity. Compared to 1D-LC approaches using the same analysis time, a 2.8-fold increase in effective peak capacity was obtained and roughly a factor 1.5 improvement in the number of identified peptides and proteins by MS/MS. Method optimization, including column dimensions (e.g. low-flow rates setups), selectivity coupling, repeatability, and computer-aided method development will be the objective of further studies.

Associated content

Supporting Information:

Details regarding the sample preparation, instrumental settings, data processing protocols, several figures displaying additional experimental data.

CRediT authorship contribution statement

Rick S. van den Hurk: Conceptualization, Methodology, Investigation, Formal Analysis, Writing – Original draft, Visualization. **Bart Lagerwaard:** Conceptualization, Methodology, Investigation, Formal Analysis, Visualization. **Mingzhe Sun:** Investigation, Formal Analysis**. Nathan J. Terlouw:** Investigation, Formal Analysis**. Job Tieleman:** Investigation, Formal Analysis**. Anniek Verstegen:** Investigation, Formal Analysis. **Bob W.J. Pirok:** Writing – review & editing, Methodology, Project administration, Supervision, Resources. **Saer Samanipour:** Writing – review & editing, Resources. **Andrea F.G. Gargano:** Conceptualization, Methodology, Investigation, Writing – review & editing, Project administration, Supervision, Resources.

Notes

The authors declare no competing financial interest.

Acknowledgements

RH Acknowledges the PARADISE project (ENPPS.TA.019.001) and received funding from the Dutch Research Council (NWO) in the framework of the Science PPP Fund for the top sectors and from the Ministry of Economic Affairs of the Netherlands in the framework of the "PPS Toeslagregeling". Moreover, Stef Molenaar is acknowledged for developing a new customized version of the MOREPEAKS software with added functionality for parallel gradient retention modelling. Denice van Herwerden is acknowledged for performing non-targeted feature detection using SAFD on a subset of the LC×LC data.

References

[1] A.P. Drabovich, M.P. Pavlou, I. Batruch, E.P. Diamandis, Proteomic and Mass

Spectrometry Technologies for Biomarker Discovery, in: Proteomic Metabolomic Approaches to Biomark. Discov., Elsevier, 2013: pp. 17–37. https://doi.org/10.1016/B978-0-12-394446-7.00002-9.

[2] E.J. Dupree, M. Jayathirtha, H. Yorkey, M. Mihasan, B.A. Petre, C.C. Darie, A Critical Review of Bottom-Up Proteomics: The Good, the Bad, and the Future of This Field, Proteomes. 8 (2020) 14. https://doi.org/10.3390/proteomes8030014.

[3] S.R. Shuken, An Introduction to Mass Spectrometry-Based Proteomics, J. Proteome Res. (2023). https://doi.org/10.1021/acs.jproteome.2c00838.

[4] D.R. Stoll, H.R. Lhotka, D.C. Harmes, B. Madigan, J.J. Hsiao, G.O. Staples, High resolution two-dimensional liquid chromatography coupled with mass spectrometry for robust and sensitive characterization of therapeutic antibodies at the peptide level, J. Chromatogr. B Anal. Technol. Biomed. Life Sci. 1134–1135 (2019) 121832. https://doi.org/10.1016/j.jchromb.2019.121832.

[5] E. Shishkova, A.S. Hebert, J.J. Coon, Now, More Than Ever, Proteomics Needs Better Chromatography, Cell Syst. 3 (2016) 321–324. https://doi.org/10.1016/j.cels.2016.10.007.

[6] J.C. Giddings, Maximum number of components resolvable by gel filtration and other elution chromatographic methods, Anal. Chem. 39 (1967) 1027–1028. https://doi.org/10.1021/ac60252a025.

[7] T. Köcher, R. Swart, K. Mechtler, Reveals a Linear Relation between Peak Capacity and Number, Anal. Chem. 83 (2011) 2699–2704. https://doi.org/10.1021/ac103243t.

[8] B.W.J. Pirok, D.R. Stoll, P.J. Schoenmakers, Recent Developments in Two-Dimensional Liquid Chromatography: Fundamental Improvements for Practical Applications, Anal. Chem. 91 (2019) 240–263.

https://doi.org/10.1021/acs.analchem.8b04841.

[9] B.W.J. Pirok, A.F.G. Gargano, P.J. Schoenmakers, Optimizing separations in online comprehensive two-dimensional liquid chromatography, J. Sep. Sci. 41 (2018) 68–98. https://doi.org/10.1002/jssc.201700863.

[10] D.R. Stoll, P.W. Carr, Two-Dimensional Liquid Chromatography: A State of the Art Tutorial, Anal. Chem. 89 (2017) 519–531. https://doi.org/10.1021/acs.analchem.6b03506.

[11] B.W.J. Pirok, P.J. Schoenmakers, Practical Approaches to Overcome the Challenges of Comprehensive Two-Dimensional Liquid Chromatography, LCGC Eur. 31 (2018) 242–249. https://www.chromatographyonline.com/view/practical-approaches-overcome-challenges-comprehensive-two-dimensional-liquid-chromatography.

[12] S. Chapel, F. Rouvière, P. Guibal, D. Mathieu, S. Heinisch, Development of a sub-hour on-line comprehensive cation exchange chromatography x RPLC method hyphenated to HRMS for the characterization of lysine-linked antibody-drug conjugates, Talanta. 240 (2022) 1–9. https://doi.org/10.1016/j.talanta.2021.123174.

[13] S. Chapel, F. Rouvière, S. Heinisch, Pushing the limits of resolving power and analysis time in on-line comprehensive hydrophilic interaction x reversed phase liquid chromatography for the analysis of complex peptide samples, J. Chromatogr. A. 1615 (2020) 460753. https://doi.org/10.1016/j.chroma.2019.460753.

[14] E. Sommella, E. Salviati, F. Merciai, M. Manfra, A. Bertamino, F. Gasparrini, E. Novellino, P. Campiglia, Online comprehensive hydrophilic interaction chromatography × reversed phase liquid chromatography coupled to mass spectrometry for in depth peptidomic profile of microalgae gastro-intestinal digests, J. Pharm. Biomed. Anal. 175 (2019) 112783. https://doi.org/10.1016/j.jpba.2019.112783.

[15] E. Sommella, E. Salviati, S. Musella, V. Di Sarno, F. Gasparrini, P. Campiglia, Comparison of online comprehensive hilic × rp and rp × rp with trapping modulation coupled to mass spectrometry for microalgae peptidomics, Separations. 7 (2020) 1–12. https://doi.org/10.3390/separations7020025.

[16] L.S. Roca, A.F.G. Gargano, P.J. Schoenmakers, Development of comprehensive two-dimensional low-flow liquid-chromatography setup coupled to high-resolution mass spectrometry for shotgun proteomics, Anal. Chim. Acta. 1156 (2021) 338349. https://doi.org/10.1016/j.aca.2021.338349.

[17] P. Yu, S. Petzoldt, M. Wilhelm, D.P. Zolg, R. Zheng, X. Sun, X. Liu, G. Schneider, A. Huhmer, B. Kuster, Trimodal Mixed Mode Chromatography That Enables E ffi cient O ffl ine Two-Dimensional Peptide Fractionation for Proteome Analysis, Anal. Chem. 89 (2017) 8884–8891. https://doi.org/https://doi.org/10.1021/acs.analchem.7b01356.

[18] D. Yeung, B. Mizero, D. Gussakovsky, N. Klaassen, Y. Lao, V. Spicer, O. V Krokhin, Separation Orthogonality in Liquid Chromatography − Mass Spectrometry for Proteomic Applications: Comparison of 16 Different Two-Dimensional Combinations, Anal. Chem. 92 (2020) 3904–3912. https://doi.org/10.1021/acs.analchem.9b05407.

[19] R.S. van den Hurk, M. Pursch, D.R. Stoll, B.W.J. Pirok, Recent trends in two-dimensional liquid chromatography, Trends Anal. Chem. (2023) 117166. https://doi.org/10.1016/j.trac.2023.117166.

[20] M. Sarrut, F. Rouvière, S. Heinisch, Theoretical and experimental comparison of one dimensional versus on-line comprehensive two dimensional liquid chromatography for optimized sub-hour separations of complex peptide samples, J. Chromatogr. A. 1498 (2017) 183–195. https://doi.org/10.1016/j.chroma.2017.01.054.

[21] D.R. Stoll, H.R. Lhotka, D.C. Harmes, B. Madigan, J.J. Hsiao, G.O. Staples, High

resolution two-dimensional liquid chromatography coupled with mass spectrometry for robust and sensitive characterization of therapeutic antibodies at the peptide level, J. Chromatogr. B Anal. Technol. Biomed. Life Sci. 1134–1135 (2019) 121832. https://doi.org/10.1016/j.jchromb.2019.121832.

[22] S. Chapel, F. Rouvière, S. Heinisch, Sense and nonsense of shifting gradients in on-line comprehensive reversed-phase LC × reversed-phase LC, J. Chromatogr. B Anal. Technol. Biomed. Life Sci. 1212 (2022). https://doi.org/10.1016/j.jchromb.2022.123512.

[23] C. Gunnarson, T. Lauer, H. Willenbring, E. Larson, M. Dittmann, K. Broeckhoven, D.R. Stoll, Implications of dispersion in connecting capillaries for separation systems involving post-column flow splitting, J. Chromatogr. A. 1639 (2021). https://doi.org/10.1016/j.chroma.2021.461893.

[24] F. Cacciola, P. Jandera, Z. Hajdú, P. Česla, L. Mondello, Comprehensive two-dimensional liquid chromatography with parallel gradients for separation of phenolic and flavone antioxidants, J. Chromatogr. A. 1149 (2007) 73–87. https://doi.org/10.1016/j.chroma.2007.01.119.

[25] P. Jandera, P. Česla, T. Hájek, G. Vohralík, K. Vyňuchalová, J. Fischer, Optimization of separation in two-dimensional high-performance liquid chromatography by adjusting phase system selectivity and using programmed elution techniques, J. Chromatogr. A. 1189 (2008) 207–220. https://doi.org/10.1016/j.chroma.2007.11.053.

[26] P. Česla, T. Hájek, P. Jandera, Optimization of two-dimensional gradient liquid chromatography separations, J. Chromatogr. A. 1216 (2009) 3443–3457. https://doi.org/10.1016/j.chroma.2008.08.111.

[27] A.A. Aly, M. Muller, A. de Villiers, B.W.J. Pirok, T. Górecki, Parallel gradients in

comprehensive multidimensional liquid chromatography enhance utilization of the separation space and the degree of orthogonality when the separation mechanisms are correlated, J. Chromatogr. A. 1628 (2020) 461452. https://doi.org/10.1016/j.chroma.2020.461452.

[28] W.C. Byrdwell, H.K. Kotapati, R. Goldschmidt, P. Jakubec, L. Nováková, Three-dimensional liquid chromatography with parallel second dimensions and quadruple parallel mass spectrometry for adult/infant formula analysis, J. Chromatogr. A. 1661 (2022) 462682. https://doi.org/10.1016/j.chroma.2021.462682.

[29] T. Ikegami, T. Hara, H. Kimura, H. Kobayashi, K. Hosoya, K. Cabrera, N. Tanaka, Two-dimensional reversed-phase liquid chromatography using two monolithic silica C18 columns and different mobile phase modifiers in the two dimensions, J. Chromatogr. A. 1106 (2006) 112–117. https://doi.org/10.1016/j.chroma.2005.10.068.

[30] K. Shoykhet, D. Stoll, S. Buckenmaier, Constant pressure mode of operation in the second dimension of two-dimensional liquid chromatography: A proof of concept, J. Chromatogr. A. 1639 (2021) 461880. https://doi.org/10.1016/j.chroma.2021.461880.

[31] P.F. Doubleday, L. Fornelli, N.L. Kelleher, Elucidating Proteoform Dynamics Underlying the Senescence Associated Secretory Phenotype, J. Proteome Res. 19 (2020) 938–948. https://doi.org/10.1021/acs.jproteome.9b00739.

[32] L.S. Roca, S.E. Schoemaker, B.W.J. Pirok, A.F.G. Gargano, P.J. Schoenmakers, Accurate modelling of the retention behaviour of peptides in gradient-elution hydrophilic interaction liquid chromatography, J. Chromatogr. A. 1614 (2020) 460650. https://doi.org/10.1016/j.chroma.2019.460650.

[33] M.J. den Uijl, P.J. Schoenmakers, G.K. Schulte, D.R. Stoll, M.R. van Bommel, B.W.J. Pirok, Measuring and using scanning-gradient data for use in method optimization for

liquid chromatography, J. Chromatogr. A. 1636 (2021) 461780. https://doi.org/10.1016/j.chroma.2020.461780.

[34] S.R.A. Molenaar, P.J. Schoenmakers, B.W.J. Pirok, MOREPEAKS, (2021). https://doi.org/10.5281/zenodo.5710442.

[35] R.J. Vonk, A.F.G. Gargano, E. Davydova, H.L. Dekker, S. Eeltink, L.J. De Koning, P.J. Schoenmakers, Comprehensive two-dimensional liquid chromatography with stationary-phase-assisted modulation coupled to high-resolution mass spectrometry applied to proteome analysis of saccharomyces cerevisiae, Anal. Chem. 87 (2015) 5387–5394. https://doi.org/10.1021/acs.analchem.5b00708.

[36] A.F.G. Gargano, M. Duffin, P. Navarro, P.J. Schoenmakers, Reducing Dilution and Analysis Time in Online Comprehensive Two-Dimensional Liquid Chromatography by Active Modulation, Anal. Chem. 88 (2016) 1785–1793. https://doi.org/10.1021/acs.analchem.5b04051.

[37] X. Li, D.R. Stoll, P.W. Carr, Equation for peak capacity estimation in two-dimensional liquid chromatography, Anal. Chem. 81 (2009) 845–850. https://doi.org/10.1021/ac801772u.

[38] L.W. Potts, D.R. Stoll, X. Li, P.W. Carr, The impact of sampling time on peak capacity and analysis speed in on-line comprehensive two-dimensional liquid chromatography, J. Chromatogr. A. 1217 (2010) 5700–5709. https://doi.org/10.1016/j.chroma.2010.07.009.

[39] H.J. Cortes, B. Winniford, J. Luong, M. Pursch, Comprehensive two dimensional gas chromatography review, J. Sep. Sci. 32 (2009) 883–904. https://doi.org/10.1002/jssc.200800654.

[40] M. Gilar, P. Olivova, A.E. Daly, J.C. Gebler, Orthogonality of separation in two-

598 dimensional liquid chromatography, Anal. Chem. 77 (2005) 6426–6434.
599 https://doi.org/10.1021/ac050923i.

600

601

602 Figure for table of contents only

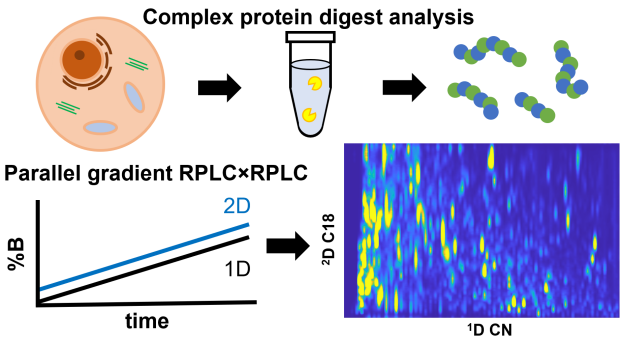

603